HHS Public Access

Author manuscript

Nature. Author manuscript; available in PMC 2015 November 28.

Published in final edited form as:

Nature. 2015 May 28; 521(7553): 529–532. doi:10.1038/nature14457.

Coordinated regulation of bidirectional COPI transport at the Golgi by cdc42

Seung-Yeol Park[1], **Jia-Shu Yang**[1], **Angela B. Schmider**[2], **Roy J. Soberman**[2,3], and **Victor W. Hsu**[1,4]

[1]Division of Rheumatology, Immunology and Allergy, Brigham and Women's Hospital, and Department of Medicine, Harvard Medical School, Boston, MA 02115 USA

[2]Nephrology Division and Department of Medicine, Massachusetts General Hospital, Charlestown, MA 02129 USA

[3]Molecular Imaging Core, Massachusetts General Hospital, Charlestown, MA 02129 USA

Abstract

The Golgi complex plays a central role in the intracellular sorting of secretory proteins [1,2]. Anterograde transport through the Golgi has been explained by the movement of Golgi cisternae, known as cisternal maturation [3–5]. Because this explanation is now appreciated to be incomplete [6], interest has developed in understanding tubules that connect the Golgi cisternae [7–9]. Here, we find that the Coat Protein I (COPI) complex sorts anterograde cargoes into these tubules. Moreover, the small GTPase cdc42 regulates bidirectional Golgi transport by targeting the dual functions of COPI in cargo sorting and carrier formation. Cdc42 also directly imparts membrane curvature in promoting COPI tubule formation. Our findings further reveal that COPI tubular transport complements cisternal maturation in explaining how anterograde Golgi transport is achieved, and that bidirectional COPI transport is modulated by environmental cues through cdc42.

In addition to its known role in generating vesicles [10], we recently discovered that COPI also generates tubules that connect the Golgi stacks [9]. However, whether these tubules act passively or actively in cargo transport has been unclear. Active transport involves coat proteins binding to cargoes. Thus, we initially examined whether COPI binds to a temperature-sensitive form of the vesicular stomatitis virus G protein (referred hereon as VSVG), which has been widely used to track anterograde Golgi transport [6–9]. We found that coatomer, the core components of the COPI complex [10], binds directly to the cytoplasmic tail of VSVG (Fig 1a and Extended data Figure. 1a). Further defining this binding, we found that coatomer binds to the membrane proximal region of the VSVG tail (Fig 1b and Extended data Figure. 1b), and then identified residues within this region critical for binding by coatomer (Fig 1c and Extended data Figure. 1a).

---

[4]Address correspondence to: Victor Hsu, Tel: 617-525-1103, vhsu@research.bwh.harvard.edu.

AUTHOR CONTRIBUTIONS

SYP, JSY, and ABS performed the experiments. VWH, SYP, RJS, and ABS designed the experiments and wrote the paper.

The authors declare no competing financial interests.

Coatomer has been shown previously to promote the retrograde transport of cargoes, such as Wbp1 [11] and the KDEL receptor [12], which involves binding to their carboxyl terminus that contains di-lysine residues. In contrast, the basic residues in VSVG recognized by coatomer are situated away from this end (see Extended data Figure. 1a), suggesting a new mode of cargo recognition by coatomer. As confirmation, we performed competition studies, and verified that a peptide derived from Wbp1 (containing the retrograde di-lysine motif) cannot compete with the VSVG tail for binding to coatomer (Fig 1d). We also employed fluorescence lifetime imaging microscopy (FLIM) to confirm that coatomer interacts with VSVG at the Golgi, and the interaction requires critical basic residues in VSVG (Fig 1e and Extended data Figure. 1c). Subsequently, we found that mutation of these basic residues delayed the transport of VSVG from the endoplasmic reticulum (ER) to the trans-Golgi (Fig 1f and Extended data Figure. 1d), but not from the ER to the cis-Golgi (Extended data Figure. 1e). Thus, coatomer promotes the intra-Golgi transport of VSVG through cargo binding.

We next examined another anterograde cargo, the endogenous low-density lipoprotein receptor (LDLR). Coatomer also binds direct to its cytoplasmic tail (Fig 2a), which also is not affected by the presence of the Wbp1 peptide (Fig 2b). As the LDLR tail also contains basic residues away from the carboxyl terminus (Extended data Figure. 2a), we next targeted them for mutagenesis and found that binding to the LDLR tail by coatomer became reduced (Fig 2a). To confirm the functional role of this binding, we swapped the tails of LDLR and VSVG, and then examined the transport of the resulting chimera (VSVG-LDLR). When critical basic residues in the LDLR tail were mutated, we observed delayed transport of VSVG-LDLR from the ER to the trans-Golgi (Fig 2c and Extended data Figure. 2b), but not from the ER to the cis-Golgi (Extended data Figure. 2c).

As compared to VSVG, VSVG-LDLR is transported slower from the ER to the cis-Golgi (Extended data Figures. 1e and 2c), and also through the Golgi (Fig 2d and Extended data Figure. 2d). Pursuing the latter observation, we found that coatomer binds more efficiently to the VSVG tail than the LDLR tail, both in vitro (Fig 2e) and in cells (Fig 2f and Extended data Figure. 3a). Moreover, mutating critical basic residues in either cargo tail results in transport rates becoming similar (Fig 2d and Extended data Figure. 2d). Furthermore, mutating a residue in VSVG that partially reduces its binding by coatomer (H494A in Fig 1c) moderately reduces VSVG transport through the Golgi (Extended data Figure. 3b). Thus, the collective results further confirmed that binding of anterograde cargoes by coatomer promotes their transport through the Golgi.

We then sought to address a key question: How can the same coat complex promote opposing directions of Golgi transport while also maintaining specificity in cargo sorting? As a clue, we noted that cdc42 has been found previously to interact with coatomer [13]. Moreover, a point mutation in cdc42 (F28L), which promotes the rapid cycling of its GTPase cycle, enhances VSVG transport [13]. We initially defined more precisely that active cdc42 (F28L) promotes the intra-Golgi segment of VSVG transport (Fig 3a and Extended data Figure. 4a), with siRNA against cdc42 (Extended data Figure. 4b) having the opposite effect (Extended data Figure. 4c). In contrast, no effect was seen on transport from the ER to the cis-Golgi (Extended data Figures. 4d and 4e). We then considered that COPI tubular

transport at the Golgi requires cPLA2α activity [9]. Targeting this activity through siRNA, we found that cdc42 can no longer promote the anterograde transport of VSVG through the Golgi (Fig 3b and Extended data Figure. 5a). Next, examining retrograde COPI vesicular transport, as tracked through a model cargo (VSVG-KDELR [9,14,15]), we found that active cdc42 (F28L) inhibits this transport (Fig 3c and Extended data Figure. 5b), while siRNA against cdc42 enhances this transport (Extended data Figure. 5c). Thus, the collective results revealed that cdc42 has opposite effects on the two directions of COPI transport at the Golgi, promoting anterograde tubular transport and inhibiting retrograde vesicular transport.

We then sought to elucidate how cdc42 exerts these effects. We had previously found that retrograde cargoes are preferentially sorted into COPI vesicles generated through a reconstitution system [9]. However, reconstituted COPI tubules contain both anterograde and retrograde cargoes [9]. Thus, to explore whether cdc42 acts to specify cargo sorting into these tubules, we added cdc42 to the reconstitution system. Remarkably, the level of a retrograde cargo (VSVG-KDELR) in COPI tubules became reduced (Fig 3d), while that of an anterograde cargo (VSVG) was unaffected (Fig 3e). In considering how cdc42 achieves these effects, we noted that cdc42 possesses a di-lysine motif, which competes with retrograde cargoes for binding to coatomer [13]. Pursuing this clue, we found that active cdc42 prevents coatomer from binding to the retrograde cargo (KDELR) tail (Fig 3f), but not coatomer binding to the anterograde cargo (VSVG) tail (Fig 3g). These results were further confirmed by FLIM (Extended data Figures. 5d and 5e). We also examined a battery of other small GTPases known to act in Golgi transport, and found that none of them affects coatomer binding to either the VSVG tail (Extended data Figure. 6a) or the KDELR tail (Extended data Figure. 6b). Other Rho small GTPases also did not have an effect (Extended data Figures. 6a and 6b). Thus, the collective results suggested that cdc42 imparts specificity in cargo sorting into COPI tubules by competing with retrograde, but not anterograde, cargoes for binding to coatomer.

Besides cargo sorting, the other major function of coat proteins is the generation of transport carriers. Previously, we found that the addition of cPLA2α to the COPI reconstitution system diverts vesicle formation to tubule formation [9]. Remarkably, when we replaced cPLA2α with the active cdc42 (F28L), COPI tubule formation was also promoted (Fig 4a), and at the expense of vesicle formation (Fig 4b). In considering how cdc42 exerts these effects, we initially ruled out that cdc42 acts through cPLA2α, as the replacement of wild-type cPLA2α with the catalytic dead form in the COPI reconstitution system did not prevent active cdc42 from promoting tubule formation (Extended data Figure. 6c), and also inhibiting vesicle formation (Extended data Figure. 6d). To decipher a different explanation, we noted that protein factors can directly impart membrane curvature, as reflected by their ability to tubulate liposomes [16,17]. Notably, when we incubated active cdc42 (F28L) with liposomes, tubulation was observed (Figs 4c and 4d).

To elucidate how cdc42 exerts this effect, we initially considered that cdc42 is prenylated, which suggests how cdc42 can insert asymmetrically into the membrane bilayer to impart curvature. As confirmation, we found that a non-prenylated form of cdc42 cannot induce liposome tubulation (Figs 4c and 4d). We then considered that cdc42 undergoes dimerization [18], which suggested an additional possibility that it can polymerize onto

membrane to exert curvature through scaffolding. Performing mutagenesis, we identified three residues at the carboxyl terminus of cdc42, anchored by di-arginines (Extended data Figure. 7a), to be required for dimerization (Extended data Figure. 7b). When the di-arginine residues were mutated, we found that active cdc42 (F28L) can no longer tubulate liposomes (Figs 4c and 4d). As further confirmation, we found that mutating the di-arginine residues also prevents cdc42 from promoting tubule formation in the COPI reconstitution system (Fig 4e). Moreover, this mutation prevents cdc42 from promoting the intra-Golgi transport of VSVG (Fig 4f and Extended data Figure. 7c). We also considered that the di-arginine residues are closely juxtaposed to the di-lysine residues in cdc42 (Extended data Figure. 7a). Thus, we assessed whether the di-arginine residues play a role in COPI cargo sorting. However, mutation of the di-arginine residues does not prevent activated cdc42 (F28L) from interacting with coatomer (Extended data Figure. 7d). Moreover, this mutation also does not alter the ability of active cdc42 (F28L) to inhibit coatomer binding to the retrograde (KDELR) cargo (Extended data Figure. 7e). In comparison, mutating the di-lysine residues in cdc42 affects this cargo binding by coatomer (Extended data Figure. 7f). These binding results were also further confirmed in cells through FLIM (Extended data Figure. 7g).

We next considered that coatomer has been identified as a target by which cdc42 promotes cellular transformation [13]. Led by this clue, we found that serum induces similar effects as active cdc42 on bidirectional Golgi transport (Extended data Figures. 8a and 8b). Moreover, the epidermal growth factor (EGF) can replace serum in exerting these effects (Extended data Figures. 8c and 8d). In contrast, neither serum (Extended data Figure. 8e) nor EGF (Extended data Figure. 8f) affects transport from the ER to the cis-Golgi. Mechanistically, serum acts through cdc42, as the enhanced anterograde transport of VSVG (Extended data Figure. 8a) and the inhibited retrograde transport of VSVG-KDELR (Extended data Figure. 8b) are prevented upon siRNA against cdc42. This was also the case for EGF stimulation (Extended data Figures. 8c and 8d).

We then considered that the Src kinase has also been shown to promote anterograde Golgi transport [19]. Upon siRNA against Src, we found that serum can no longer modulate bidirectional Golgi transport (Extended data Figures. 9a and 9b). We also found that pharmacologic activation of Src reproduces the effects of serum (Extended data Figures. 9c and 9d). Moreover, siRNA against cdc42 prevents Src activation from exerting these effects (Extended data Figures. 9c and 9d). Thus, we concluded that a signaling cascade, which involves growth factors activating Src and then cdc42, modulates bidirectional Golgi transport (Extended data Figure. 10a). Notably, as siRNA against cPLA2α prevents the ability of Src activation to promote VSVG transport through the Golgi (Extended data Figure. 10b), we further concluded that the signaling cascade targets COPI tubular transport in promoting anterograde Golgi transport.

In summary, we have advanced a new understanding of how Golgi transport is achieved and regulated. Our findings also address an ongoing controversy regarding the role of COPI in anterograde Golgi transport. Whereas this debate has focused on the role of COPI vesicular transport [20], we provide a reconciling explanation by showing how COPI acts anterograde through tubular transport. Another notable finding is that cdc42 acts not just as a regulator of cellular events, but also as an effector, which in the case of COPI transport involves a direct

ability to impart membrane curvature. Our results also shed new insight into how cdc42 targets coatomer for cellular transformation. Whereas cdc42 was thought previously to affect COPI transport in the retrograde direction [13], our finding that cdc42 modulates bidirectional COPI transport to favor the anterograde direction suggests more readily how transformation is promoted, as the rapid growth and division of tumors is predicted to require enhanced secretion.

METHODS

Chemicals, lipids, peptides, and cells

The src family activator (Santa Cruz, #SC3052) has been described [19]. GDP and GTP were purchased (Sigma-Aldrich). DOPC (dioleoylphosphocholine), DOPE (dioleoylphosphatidylethanolamine), DOPS (dioleoylphosphatidylserine), PA (phosphatidic acid) and cholesterol were also purchased (Avanti Polar Lipid). Peptides encoding the Wbp1 tail (wild-type, KKLETFKKTN; mutant, KKLETFSSTN) were synthesized (GenScript). Culturing of HeLa cells have been described [9,14,15].

Antibodies

Mouse anti-beta subunit of coatomer, anti-zeta subunit of coatomer, mouse anti-myc (9E10), sheep anti-TGN46, rabbit anti-Giantin antibodies have been described previously [21]. Rabbit anti-myc antibody (#2278S), rabbit anti-cdc42 antibody (#2462S), and mouse anti-β-actin antibody (#3700P) were obtained (Cell Signaling). All secondary antibodies were also obtained (Jackson ImmunoResearch Laboratory).

Purified and recombinant proteins

Preparation of coatomer, ARF1, ARFGAP1, BARS, cPLA2α, and Golgi membrane have been described [9,12,14]. To generate the prenylated form of human cdc42, pFASTBAC THb (Invitrogen) was used to generate baculovirus using Bac-to-Bac Baculovirus Expression system (Invitrogen). Infected Sf9 cells were suspended hypotonic buffer (20 mM sodium borate [pH 10.2], 5 mM $MgCl_2$, and protease inhibitor) followed by lysis using dounce homogenizer. Membrane bound cdc42 was collected by 150,000 × g centrifugation for 30 minutes. The pellet was then resuspended with TBS-M (50 mM Tris [pH 7.2], 150 mM NaCl, and 5 mM $MgCl_2$, and protease inhibitor), followed by centrifugation at 150,000 × g for 30 minutes. Prenylated cdc42 was solubilized from membranes using TBS-M containing 1% Triton X-100 for 1 hour, followed by centrifugation at 9,000 × g for 20 minutes. The his-tagged cdc42 was then purified from the supernatant fraction using a nickel column. Non-prenylated cdc42 was generated using bacterial expression. The last three amino acids were deleted to mimic the protein sequence of the prenylated form (see Extended data Figure. 7e). Human cdc42 in pET-15b (Novagen) was expressed in bacteria (BL21) with 100 μM of IPTG induction at 37°C for 2 hour. The his-tagged cdc42 was isolated with a nickel column, and then released with elution buffer (50 mM Tris [pH 7.2], 500 mM NaCl, 5 mM $MgCl_2$, 0.1% CHAPS, and 250 mM imidazole). Recombinant forms of Rac1, RhoA, and Rabs 1A, 2A, 6A, and 33B were generated similarly.

Plasmids

Cytoplasmic domain of cargoes fused to GST was generated using in vitro annealing. Paired oligonucleotides were annealed in buffer (30 mM HEPES-KOH, pH 7.4, 150 mM KCl, 2mM $MgCl_2$) at 90°C for 1 min followed by cooling down. Annealed duplexes were inserted into pGEX-4T-3 (GE Healthcare). GST fused cytoplasmic peptides of LDLR were generated using polymerase chain reaction. VSVG-LDLR was generated by fusing the cytoplasmic tail of LDLR to the luminal and transmembrane domains of VSVG-ts045. Mutations were generated using polymerase chain reaction or QuikChange Site-Directed-Mutagenesis (Strategene). VSVG-ts045 and VSVG-ts045-KDELR have been described previously [21]. Cdc42, F28L mutant, and di-lysine mutant of F28L in pFASTBAC THb and PKH3 were gifts from Dr. Richard A. Cerione (Cornell University). Di-arginine mutant of cdc42 was generated using polymerase chain reaction with paired oligonucleotides. Additional plasmids were obtained and then subcloned into pET-15b to generate recombinant proteins: Rac1 and RhoA (Danny Manor, Case Western Reserve University), Rab1A, 2A, and 6A (David Lambright, University of Massachusetts), and Rab33B (Mitsunori Fukuda, Tohoku University). See supplementary information for details on the oligonucleotides used to generate chimeric constructs and point mutations.

Transfections and siRNA

Transfection of DNA plasmids was performed using FuGene6 (Roche). Transfection of siRNA was carried out using Lipofectamine® RNAiMAX (Invitrogen). The siRNA sequence against cPLA2α has been described previously [9]. The siRNA sequences used to target human cdc42 (5′-GATAACTCACCACTGTCCA -3′) and human Src (5′-TGTTCGGAGGCTTCAACTCCT-3′) were obtained (Dharmacon). Point mutations in cdc42 to render siRNA resistant were generated using oligonucleotides (5′-GAAAAGTGGGTGCCTGAGATAACTCATCACTGTCCAAAGACTCCTTTCTTGCTT GTT GGG -3′ and 5′-CCCAACAAGCAAGAAAGGAGTCTTTGGACAGTGATGAGTTATCTCAGGCACCCA CT TTTC -3′).

In vitro binding assays

GST fusions were expressed in bacteria (BL21 cell) with ITPG induction. After lysis in buffer (20 mM Tris [pH 8.0], 100 mM NaCl, 1mM EDTA, 1% Triton X-100, 1 mg/ml of lysozyme and protease inhibitor), GST peptide was incubated with glutathione Sepharose beads (GE Healthcare). GST fusions on beads were then incubated with purified coatomer (2.5 nM) at 4°C for 1 hour in incubation buffer (25 mM Hepes [pH 7.2], 50 mM KCl, 2.5 mM $Mg(OAc)_2$, and 0.5% NP-40). For competition experiments with peptides, GST fusions on beads were co-incubated with coatomer and peptide at 4°C for 1 hour in incubation buffer. Beads were then rinsed twice with incubation buffer and then analyzed by SDS-PAGE followed by immunoblotting or Coomassie staining. For competition experiments with small GTPases, GTPases were loaded with either GTP or GDP and then incubated with cargo (as GST fusions on beads) and coatomer. Quantitation was performed by analyzing the level of coatomer and normalizing for the level of cargo on beads.

In vivo transport assays

Anterograde transport of VSVG and retrograde transport of VSVG-KDELR has been described previously [9,21]. Briefly, Hela cells were transfected with VSVG-ts045 and VSVG-ts045-KDELR to track anterograde and retrograde transport, respectively. To track transport from the ER to the Golgi, cells were incubated at 40°C for 2 hours to accumulate a synchronized pool of VSVG at the ER. Cells were then shifted to incubation at 32°C to allow transport from the ER to proceed. To examine intra-Golgi transport, cells were incubated at 15°C incubation for 2 hours to accumulate a synchronized pool of VSVG at the pre-Golgi region, followed by shift to 32°C to allow transport through the Golgi. To study retrograde transport, cells expressing VSVG-ts045-KDELR were incubated at 32°C for 2 hours. Cells were then incubated at 40°C. This prevents further anterograde transport from the ER, and thereby allowing one round of retrograde transport from the Golgi to the ER to be assessed. In stimulation experiments, cells were starved using DMEM supplemented with 0.1% BSA for 2 hours followed by stimulation with serum or a Src activator phosphopeptide [22] (10 μM) for 1 hour. Transport was quantified by measuring (Metamorph) the colocalization of cargoes with organelle markers over time.

FLIM

Interactions were monitored using time correlated single-photon counting fluorescence lifetime image microscopy analysis (TCSPC-FLIM), which has been described previously [23,24]. Briefly, the different forms of VSVG were detected through the myc tag appended at the carboxy terminus using an anti-myc antibody. This antibody was then detected with a secondary antibody conjugated to Alexa Fluor 594 (acceptor fluorophore). Coatomer was detected with the anti-coatomer antibody. This antibody was then detected with a secondary antibody conjugated to Alexa Fluor 488 (donor fluorophore). The baseline lifetimes of the donor fluorophore were calculated by single-exponential decay fitting of fluorescence emission in the absence of the acceptor fluorophore. For samples that involved staining for both donor and acceptor, lifetimes were fitted to a bi-exponential decay with lifetime of one component fixed to the donor-only lifetime. Three variables for FLIM were determined: 1) lifetime for the interacting fraction, τ_1, 2) lifetime for the non-interacting fraction, τ_2, and 3) the percent of interacting molecules, a_1 (%). Because VSVG is transported from the ER to the Golgi, we used this mobility to define key physiologic parameters in quantifying the interaction between VSVG and coatomer (based on the τ1 values). The maximal interaction was defined by quantifying VSVG interacting with coatomer at the Golgi, and minimal interaction was defined by performing quantitation when VSVG is at the ER. Interactions of the different forms of VSVG with coatomer were then expressed as the fraction of the maximal interaction (coatomer interacting with wild-type VSVG at the Golgi).

COPI reconstitution system

The two-stage incubation system was performed as described previously [9,14]. Briefly, Golgi membrane (250 μg) was washed with 100 ul of 3M KCl for 5 minutes, and then diluted with 1 ml of reaction buffer (25 mM Hepes-KOH [pH7.2], 50 mM KCl, 2.5 mM $Mg(OAc)_2$, 1 mg/ml soybean trypsin inhibitor, 1 mg/ml BSA, and 200 mM sucrose). In the first-stage, the

washed membrane was incubated with Arf1, coatomer, and GTP at 37 °C for 10 minutes. Reaction was stopped on the ice water for 5 min, followed by centrifuged at 12,000 × g for 20 minutes. In second stage, the pellet was resuspended with reaction buffer, and then incubated with ArfGAP1 and BARS for 20 minutes to generate COPI vesicles, or additionally with cdc42 and/or cPLA2α to generate COPI tubules.

Liposome tubulation assay

Liposomes were generated using a mixture of pure lipids (Avanti Polar Lipids): DOPC (33%), DOPS (5%), DOPE (15%), PA (30%), and cholesterol (18%). Lipids (500 μg) in glass tube were evaporated under N_2 gas. Lipids were resuspended with assay buffer (25 mM Hepes [pH 7.2], 50 mM KCl, 2.5 mM $Mg(OAc)_2$, and 200 mM sucrose) and hydrated overnight. Liposomes were then passed through 400 nm filter membrane (Whatman) in a mini-extruder (Avanti Polar Lipids). Recombinant cdc42 was then incubated with liposomes at room temperature for 30 minutes, followed by EM analysis.

EM analysis

EM analysis of Golgi tubules has been described previously [9]. Briefly, membrane samples were loaded on EM grids and then fixed with 2% PFA/PBS for 10 minutes. After blocking with 1% BSA/PBS for 10 minutes, grids were rinsed with water, followed by uranyl acetate staining. Golgi tubule was detected using JEOL 1200EX Transmission electron microscope. To detect cargoes in the reconstituted tubules, immunogold labeling was performed, which involved incubation with mouse anti-Myc antibody (9E10) for 1 hour to detect the myc-tagged form of either VSVG or VSVG-KDELR. After rinsing with PBS, the sample was incubated with a rabbit anti-mouse antibody for 30 minutes. After an additional rinse with PBS, the sample was further incubated with protein A (conjugated with 10 nm gold particles). Grids were then washed with water, followed by uranyl acetate staining, and then examination by EM. 50 EM meshes were examined for quantitation in each condition of an experiment.

Gel filtration chromatography

Dimerization of cdc42 was determined using Superdex 200 10/300 GL (GE Healthcare), essentially as previously described [18]. Recombinant cdc42 was applied at a flow rate of 0.5 ml/min and monitored by UV detector.

Extended Data

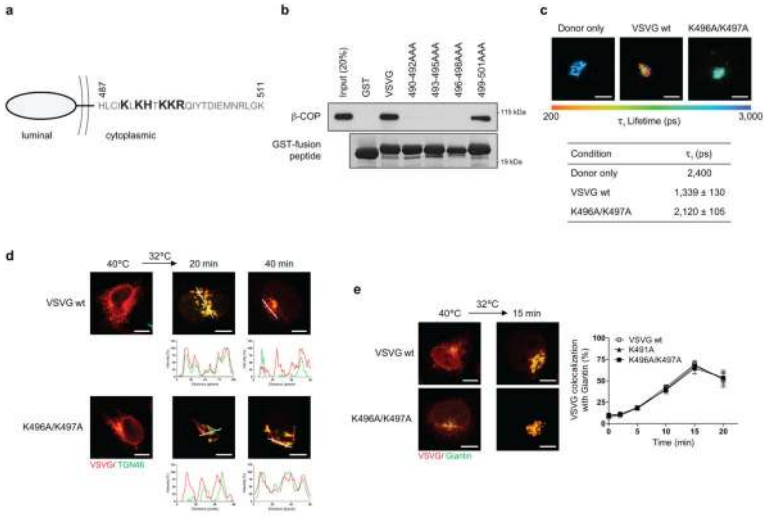

Figure 1. Characterizing VSVG transport

a, Cytoplasmic sequence of VSVG with residues critical for binding by coatomer highlighted. **b,** Effect of point mutations in the VSVG tail on the in vitro binding of this tail by coatomer, n = 5. **c**, FLIM assessing interaction between VSVG and coatomer. Representative images that are pseudo-colored based on τ_1 values are shown (out of 10), bar = 5 um. Quantitation is also shown, n = 3, mean +/− s.e.m. **d,** Effect of mutations in the VSVG tail on its transport from the ER to the trans-Golgi. Colocalization is exemplified by line scanning across representative images (out of 5), bar = 5 um. **e,** Effect of mutations in the VSVG tail on its transport from the ER to the cis-Golgi. Representative images of colocalization are shown (out of 5), bar = 5 um. Quantitation is also shown, n = 3, mean +/− s.e.m.

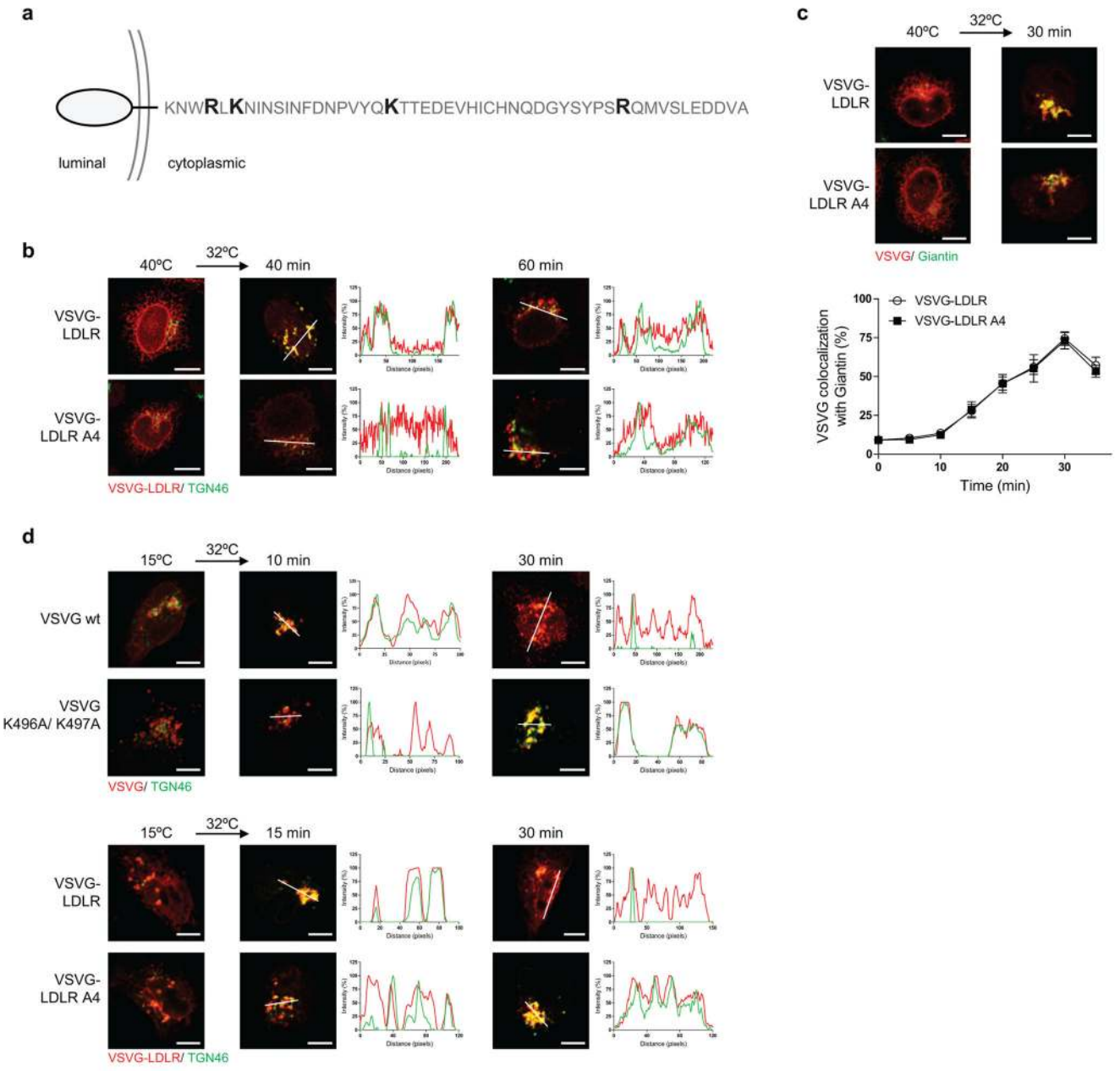

Figure 2. Characterizing VSVG-LDLR transport

a, Cytoplasmic sequence of LDLR with basic residues critical for binding by coatomer highlighted. **b,** Effect of mutations in the LDLR tail on the transport of VSVG-LDLR from the ER to the trans-Golgi. Colocalization is exemplified by line scanning across representative images (out of 5), bar = 5 um, **c,** Effect of mutations in the LDLR tail on the transport of VSVG-LDLR from the ER to the cis-Golgi. Representative images of colocalization are shown (out of 5), bar = 5 um. Quantitation is also shown, n = 4, mean +/− s.e.m., **d,** Effect of mutations in cargo tails on the intra-Golgi transport of various cargoes. Colocalization is exemplified by line scanning across representative images (out of 5), bar = 5 um.

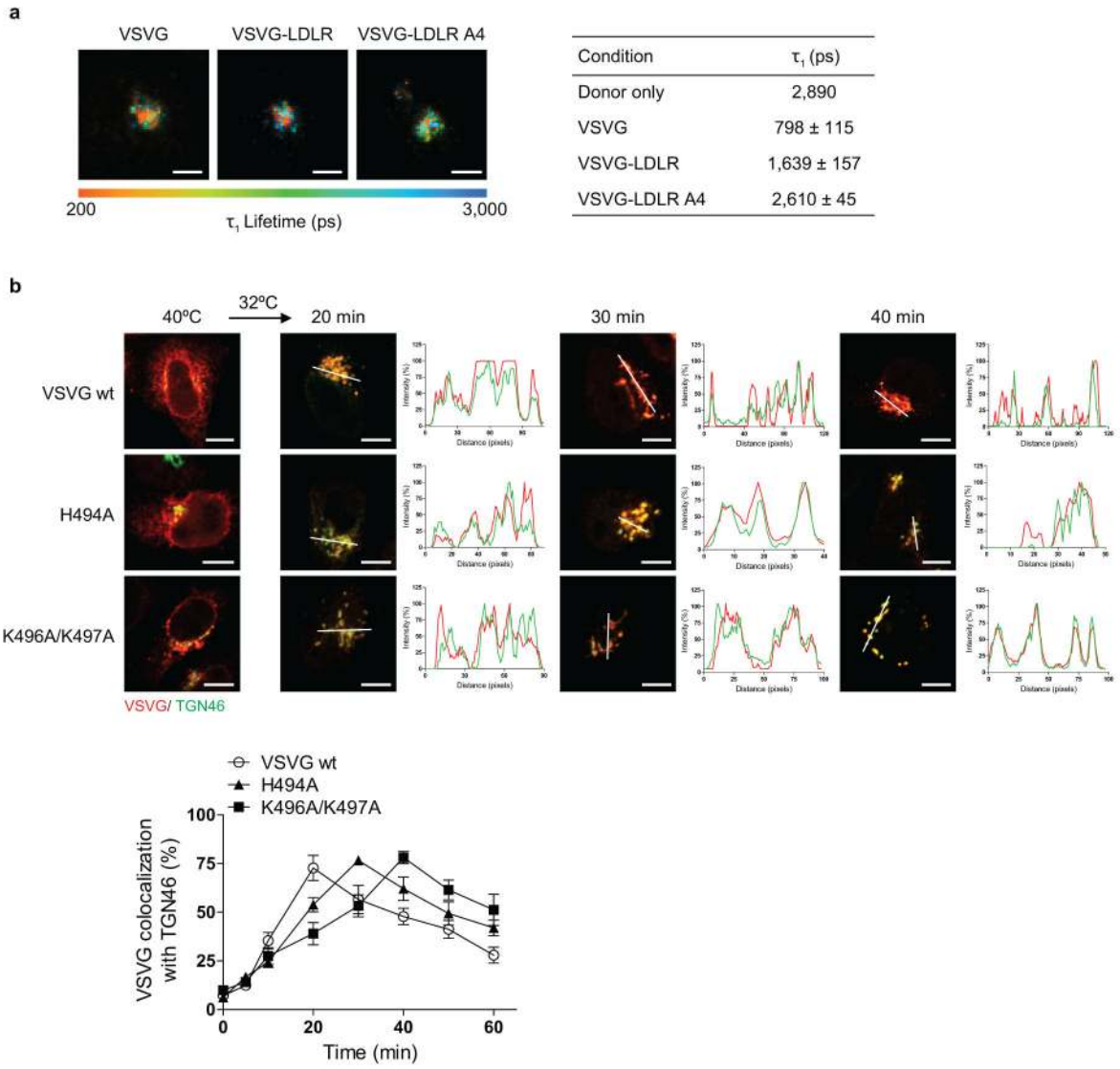

Figure 3. Further characterizing cargo transport

a, FLIM assessing interaction between different forms of VSVG and coatomer. Representative images that are pseudo-colored based on τ_1 values are shown (out of 10), bar = 5 um. Quantitation is also shown, n = 3, mean +/− s.e.m., **b,** Effect of mutations in the VSVG tail on its transport from the ER to the trans-Golgi. Colocalization is exemplified by line scanning across representative images (out of 5), bar = 5 um. Quantitation is also shown, n = 3, mean +/− s.e.m.

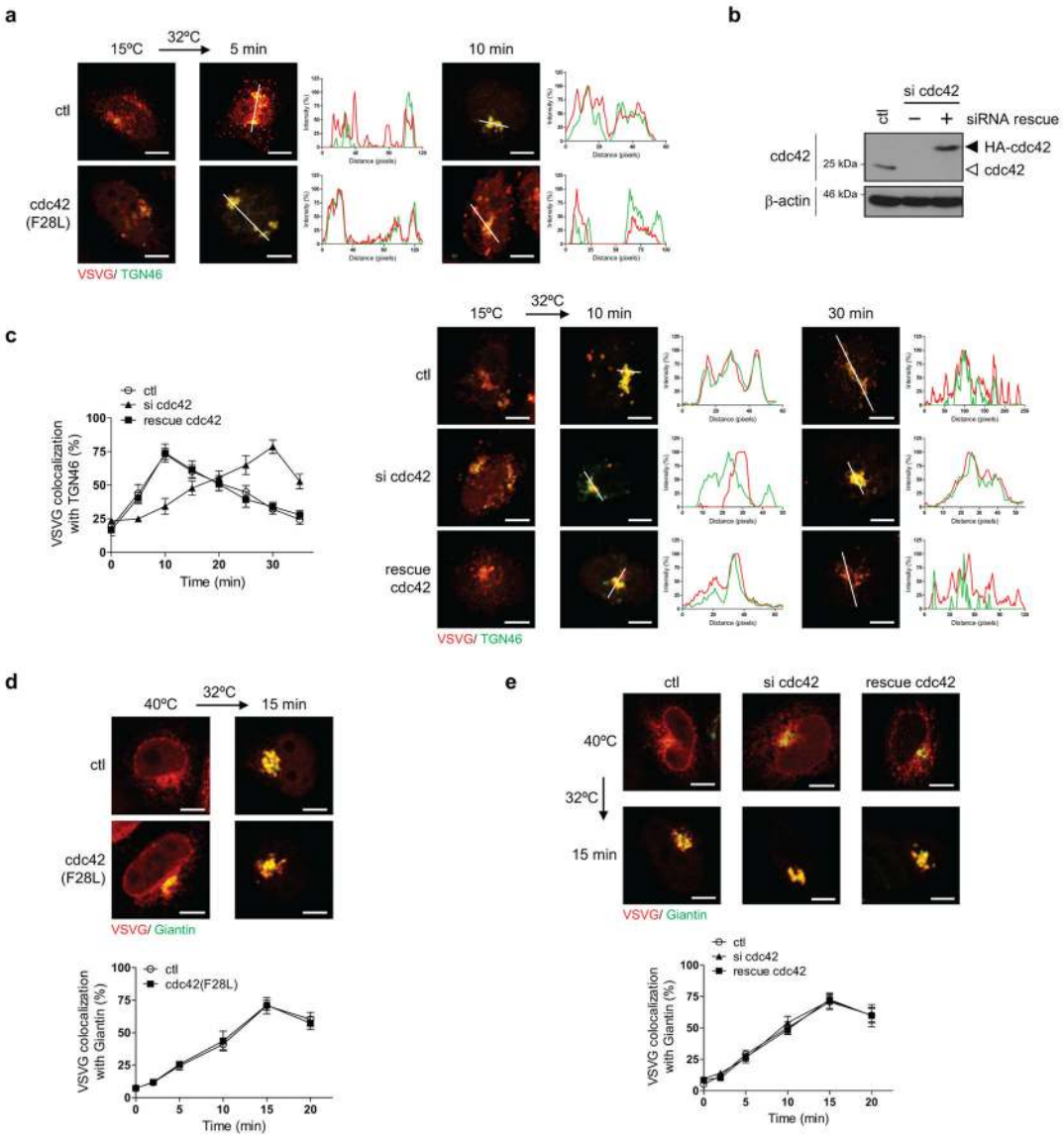

Figure 4. Characterizing how cdc42 affects VSVG transport

a, Effect of expressing active cdc42 on the intra-Golgi transport of VSVG. Colocalization is exemplified by line scanning across representative images (out of 5), bar = 5 um. **b,** Immunoblotting of whole cell lysates to assess efficiency of siRNA treatment, n = 3. **c,** Effect of siRNA against cdc42 on the intra-Golgi transport of VSVG. Colocalization is exemplified by line scanning across representative images (out of 5), bar = 5 um. Quantitation is also shown, n = 4, mean +/− s.e.m. **d,** Effect of expressing active cdc42 on VSVG transport from the ER to the cis-Golgi. Representative images of colocalization are shown (out of 5), bar = 5 um. Quantitation is also shown, n = 5, mean +/− s.e.m. **e,** Effect of siRNA against cdc42 on VSVG transport from the ER to the cis-Golgi. Representative images of colocalization are shown (out of 5), bar = 5 um. Quantitation is also shown, n = 4, mean +/− s.e.m.

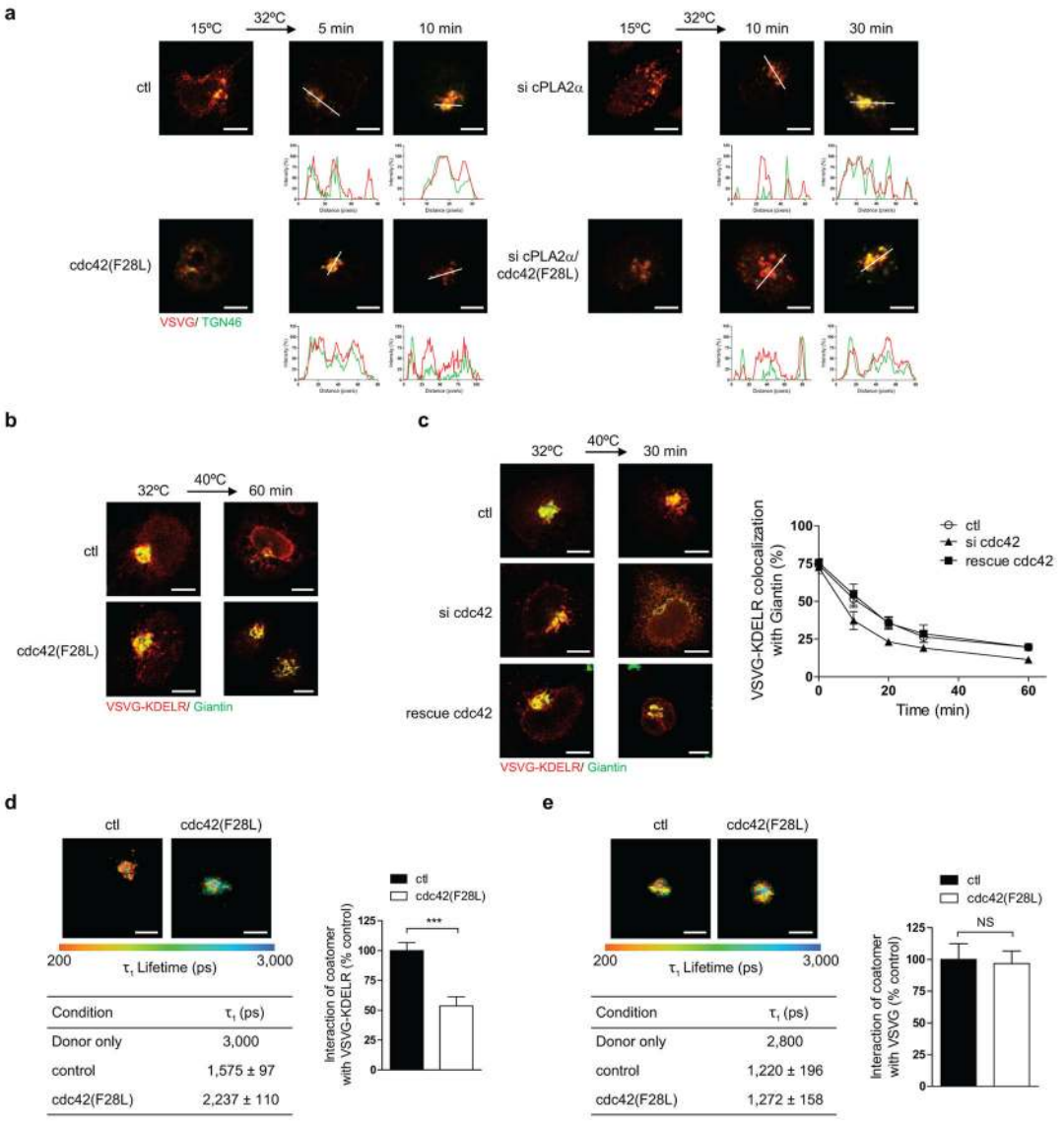

Condition	τ_1 (ps)
Donor only	3,000
control	1,575 ± 97
cdc42(F28L)	2,237 ± 110

Condition	τ_1 (ps)
Donor only	2,800
control	1,220 ± 196
cdc42(F28L)	1,272 ± 158

Figure 5. Further characterizing the effects of cdc42

a, Effect of various conditions on the intra-Golgi transport of VSVG. Colocalization is exemplified by line scanning across representative images (out of 5), bar = 5 um. **b,** Effect of expressing active cdc42 on the transport of VSVG-KDELR. Representative images of colocalization is shown (out of 5), bar = 5 um. **c,** Effect of siRNA against cdc42 on the transport of VSVG-KDELR. Representative images of colocalization are shown (out of 5), bar = 5 um. Quantitation is also shown, n = 3, mean +/− s.e.m. **d,e,** FLIM assessing the effect of active cdc42 on the interaction between different VSVG forms and coatomer. Representative images that are pseudo-colored based on τ_1 values are shown (out of 10), bar = 5 um. Quantitation is also shown as table and as graph, n= 3, mean +/− s.e.m., ***P<0.001, NS indicating non-significance (two-tailed Mann-Whitney test).

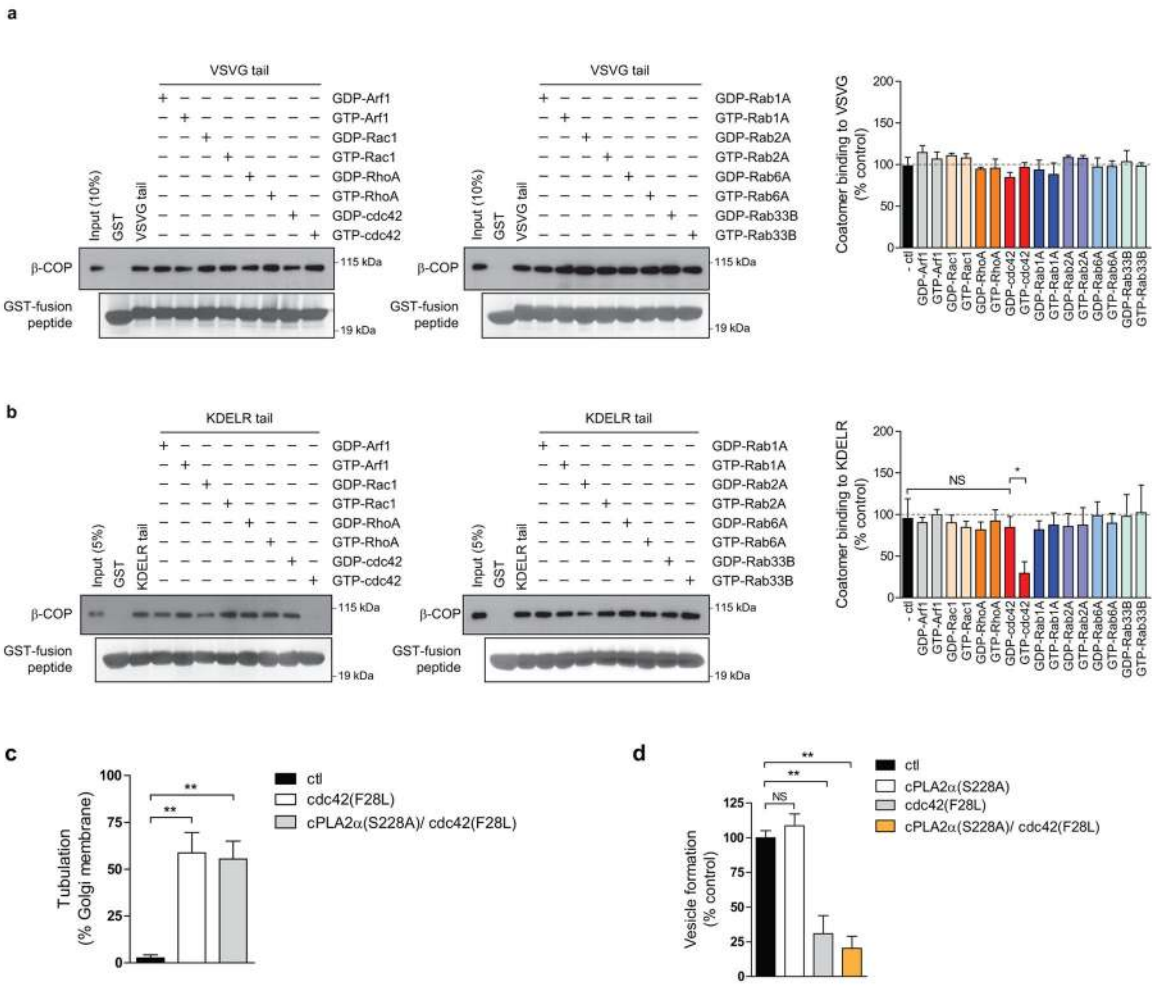

Figure 6. Characterizing how cdc42 affects COPI cargo sorting and carrier formation

a, b, Effect of different small GTPases on the in vitro binding of cargo tails by coatomer. Representative blots are shown (out of 3). Quantitation is also shown, n = 3, mean +/− s.e.m., *P<0.05, NS indicating non-significance (two-tailed Student's *t*-test). **c, d,** Effect of different active forms of cdc42 on tubule and vesicle formation in the COPI reconstitution system, n = 4, mean +/− s.e.m., **P<0.01, NS indicating non-significance (two-tailed Student's *t*-test).

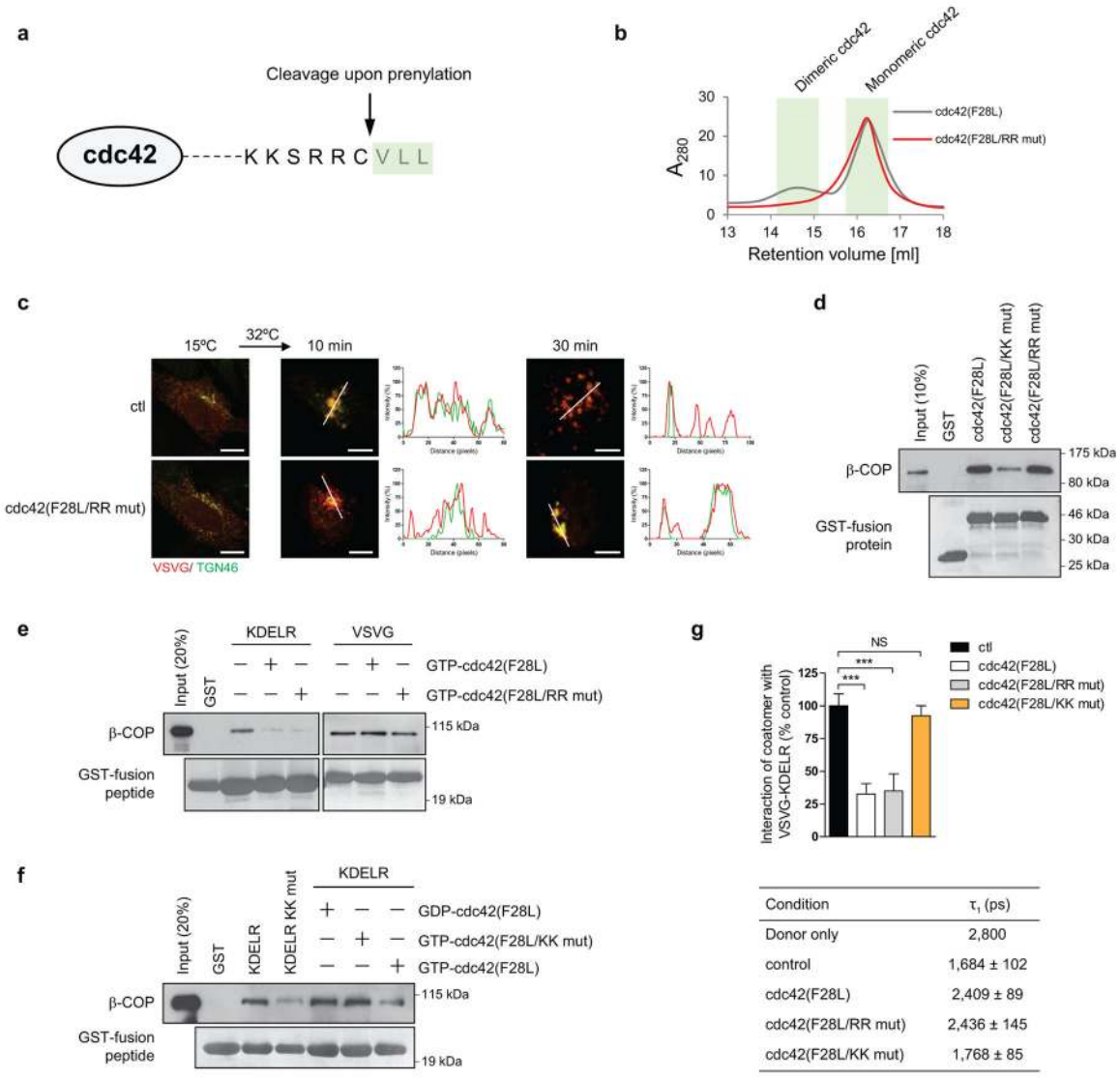

Condition	τ_1 (ps)
Donor only	2,800
control	1,684 ± 102
cdc42(F28L)	2,409 ± 89
cdc42(F28L/RR mut)	2,436 ± 145
cdc42(F28L/KK mut)	1,768 ± 85

Figure 7. Delineating the role of di-arginine residues in cdc42

a, Amino acid sequence at the carboxyl terminus of cdc42. The last three residues are cleaved upon prenylation. **b,** The di-arginine residues in cdc42 are required for cdc42 dimerization. Representative result from gel filtration (out of 2) is shown. **c,** Effect of different conditions on the intra-Golgi transport of VSVG. Colocalization is exemplified by line scanning across representative images (out of 5), bar = 5 um. **d,** Effect of mutations in cdc42 on its ability to bind coatomer in vitro. Representative blot (out of 2) is shown. **e,** Effect of mutations in cdc42 on its ability to compete with cargo tails for binding to coatomer in vitro. Representative blot (out of 3) is shown. **f,** Effect of different forms of cdc42 to compete with the KDELR tail for binding to coatomer in vitro. Representative blot (out of 2) is shown. **g**, FLIM examining VSVG-KDELR interacting with coatomer, n= 3, mean +/− s.e.m., ***P<0.001, NS indicating non-significance (two-tailed Mann-Whitney test).

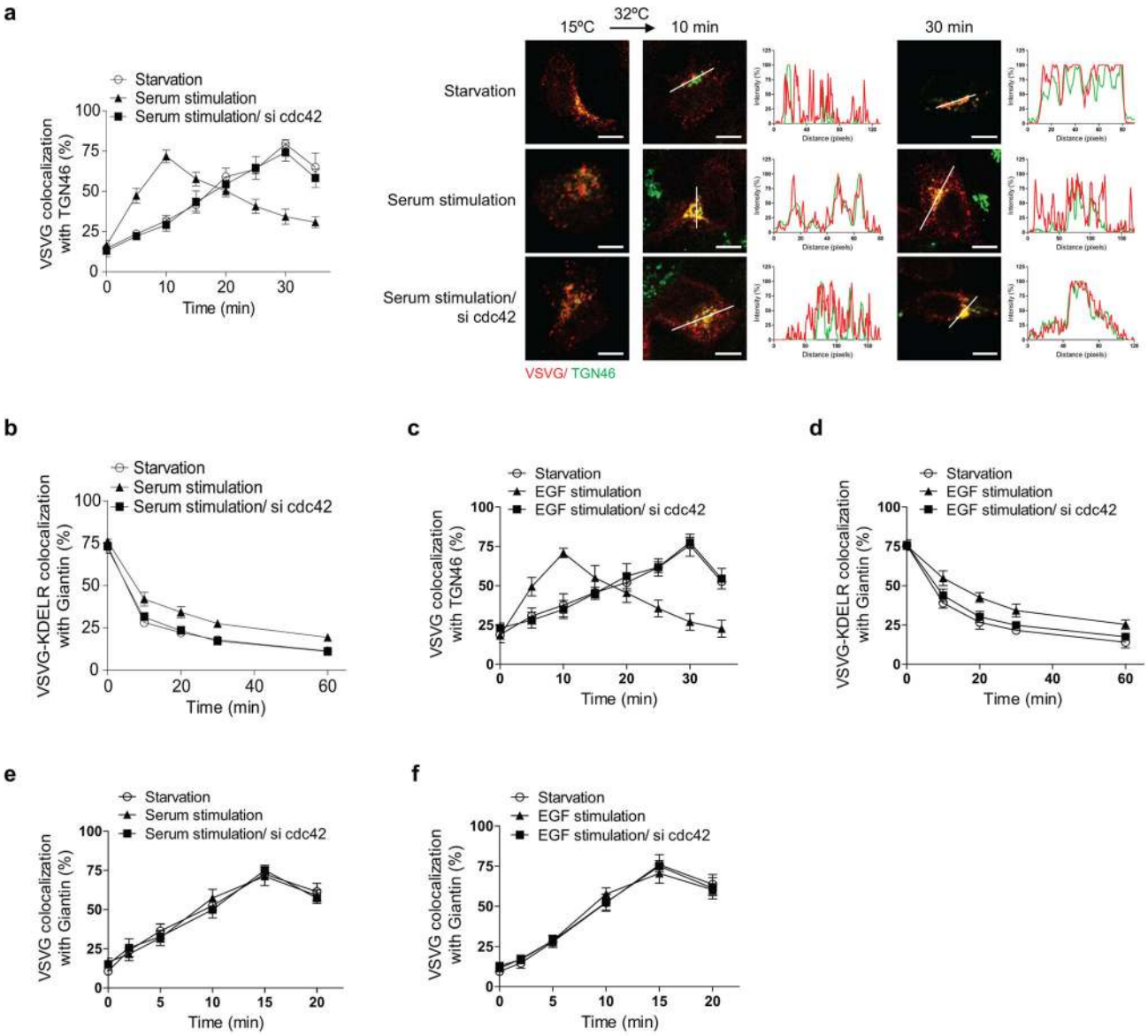

Figure 8. Delineating how external stimuli regulate bidirectional Golgi transport

a, Effect of different conditions on the intra-Golgi transport of VSVG. Colocalization is exemplified by line scanning across representative images (out of 5), bar = 5 um. Quantitation is also shown, n = 3, mean +/− s.e.m. **b,** Effect of serum on the transport of VSVG-KDELR, n = 3, mean +/− s.e.m. **c,** Effect of EGF on the intra-Golgi transport of VSVG, n = 3, mean +/− s.e.m. **d,** Effect of EGF on the transport of VSVG-KDELR, n = 3, mean +/− s.e.m. **e, f,** Effect of different conditions on VSVG transport from the ER to the cis-Golgi, n = 3, mean +/− s.e.m.

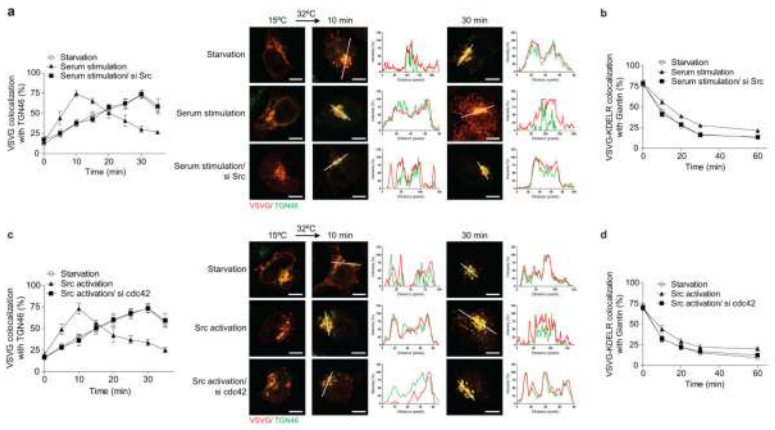

Figure 9. Delineating how Src regulates bidirectional Golgi transport

a, c, Effect of different conditions on the intra-Golgi transport of VSVG. Colocalization is exemplified by line scanning across representative images (out of 5), bar = 5 um. Quantitation is also shown, n = 3 experiments, mean +/− s.e.m. **b, d,** Effect of different conditions on the transport of VSVG-KDELR, n = 3, mean +/− s.e.m.

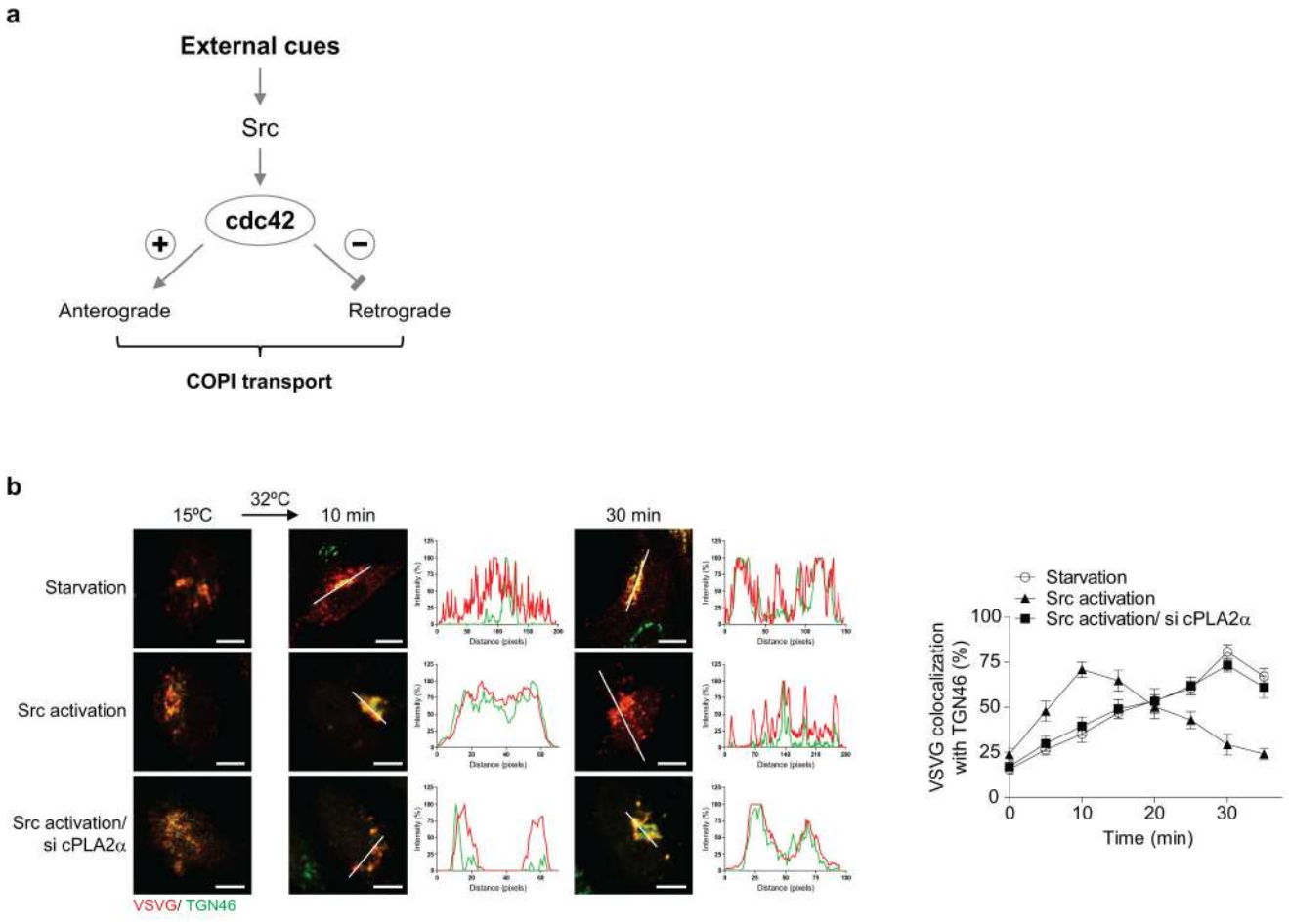

Figure 10. Further characterizing how bidirectional COPI transport at the Golgi is regulated

a, Summarizing how external stimuli regulates bidirectional COPI transport through a signaling cascade. **b,** Effect of Src activation on the intra-Golgi transport of VSVG. Colocalization is exemplified by line scanning across representative images (out of 5), bar = 5 um. Quantitation is also shown, n = 3, mean +/− s.e.m.

Supplementary Material

Refer to Web version on PubMed Central for supplementary material.

Acknowledgments

We thank Jian Li, Ming Bai, Xavier Michelet, and Claudia Alves for discussions, and Maria Ericsson for EM technical advice. This work was funded by grants from the National Institutes of Health to VWH (R01GM058615), RJS (R01AI068871 and R01AR065538), ABS (K01DK089145), and also by the Basic Science Research Program of the National Research Foundation of Korea to SYP (2014R1A6A3A03056673).

References

1. Glick BS, Nakano A. Membrane traffic within the Golgi apparatus. Annu Rev Cell Dev Biol. 2009; 25:113–132. [PubMed: 19575639]
2. Nakano A, Luini A. Passage through the Golgi. Curr Opin Cell Biol. 2010; 22:471–478. [PubMed: 20605430]
3. Bonfanti L, et al. Procollagen traverses the Golgi stack without leaving the lumen of cisternae: evidence for cisternal maturation. Cell. 1998; 95:993–1003. [PubMed: 9875853]
4. Losev E, et al. Golgi maturation visualized in living yeast. Nature. 2006; 441:1002–1006. [PubMed: 16699524]
5. Matsuura-Tokita K, Takeuchi M, Ichihara A, Mikuriya K, Nakano A. Live imaging of yeast Golgi cisternal maturation. Nature. 2006; 441:1007–1010. [PubMed: 16699523]
6. Patterson GH, et al. Transport through the Golgi apparatus by rapid partitioning within a two-phase membrane system. Cell. 2008; 133:1055–1067. [PubMed: 18555781]
7. Trucco A, et al. Secretory traffic triggers the formation of tubular continuities across Golgi sub-compartments. Nat Cell Biol. 2004; 6:1071–1081. [PubMed: 15502824]
8. San Pietro E, et al. Group IV phospholipase A(2)alpha controls the formation of inter-cisternal continuities involved in intra-golgi transport. PLoS Biol. 2009; 7:e1000194. [PubMed: 19753100]
9. Yang JS, et al. COPI acts in both vesicular and tubular transport. Nat Cell Biol. 2011; 13:996–1003. [PubMed: 21725317]
10. Hsu VW, Lee SY, Yang JS. The evolving understanding of COPI vesicle formation. Nat Rev Mol Cell Biol. 2009; 10:360–364. [PubMed: 19293819]
11. Cosson P, Letourneur F. Coatomer interaction with di-lysine endoplasmic reticulum retention motifs. Science. 1994; 263:1629–1631. [PubMed: 8128252]
12. Yang JS, et al. ARFGAP1 promotes the formation of COPI vesicles, suggesting function as a component of the coat. J Cell Biol. 2002; 159:69–78. [PubMed: 12379802]
13. Wu WJ, Erickson JW, Lin R, Cerione RA. The gamma-subunit of the coatomer complex binds Cdc42 to mediate transformation. Nature. 2000; 405:800–804. [PubMed: 10866202]
14. Yang JS, et al. A role for BARS at the fission step of COPI vesicle formation from Golgi membrane. EMBO J. 2005; 24:4133–4143. [PubMed: 16292346]
15. Yang JS, et al. A role for phosphatidic acid in COPI vesicle fission yields insights into Golgi maintenance. Nat Cell Biol. 2008; 10:1146–1153. [PubMed: 18776900]
16. Zimmerberg J, Kozlov MM. How proteins produce cellular membrane curvature. Nat Rev Mol Cell Biol. 2006; 7:9–19. [PubMed: 16365634]
17. McMahon HT, Gallop JL. Membrane curvature and mechanisms of dynamic cell membrane remodelling. Nature. 2005; 438:590–596. [PubMed: 16319878]

18. Zhang B, Zheng Y. Negative regulation of Rho family GTPases Cdc42 and Rac2 by homodimer formation. J Biol Chem. 1998; 273:25728–25733. [PubMed: 9748241]
19. Pulvirenti T, et al. A traffic-activated Golgi-based signalling circuit coordinates the secretory pathway. Nat Cell Biol. 2008; 10:912–922. [PubMed: 18641641]
20. Emr S, et al. Journeys through the Golgi--taking stock in a new era. J Cell Biol. 2009; 187:449–453. [PubMed: 19948493]
21. Bai M, et al. ARFGAP1 promotes AP-2 dependent endocytosis. Nature Cell Biol. 2011; 13:559–567. [PubMed: 21499258]
22. Lu B, et al. Peptide neurotransmitters activate a cation channel complex of NALCN and UNC-80. Nature. 2009; 457:741–744.10.1038/nature07579 [PubMed: 19092807]
23. Bair AM, Turman MV, Vaine CA, Panettieri RA Jr, Soberman RJ. The nuclear membrane leukotriene synthetic complex is a signal integrator and transducer. Mol Biol Cell. 2012; 23:4456–4464.10.1091/mbc.E12-06-0489 [PubMed: 23015755]
24. Azcutia V, et al. CD47 plays a critical role in T-cell recruitment by regulation of LFA-1 and VLA-4 integrin adhesive functions. Mol Biol Cell. 2013; 24:3358–3368.10.1091/mbc.E13-01-0063 [PubMed: 24006483]

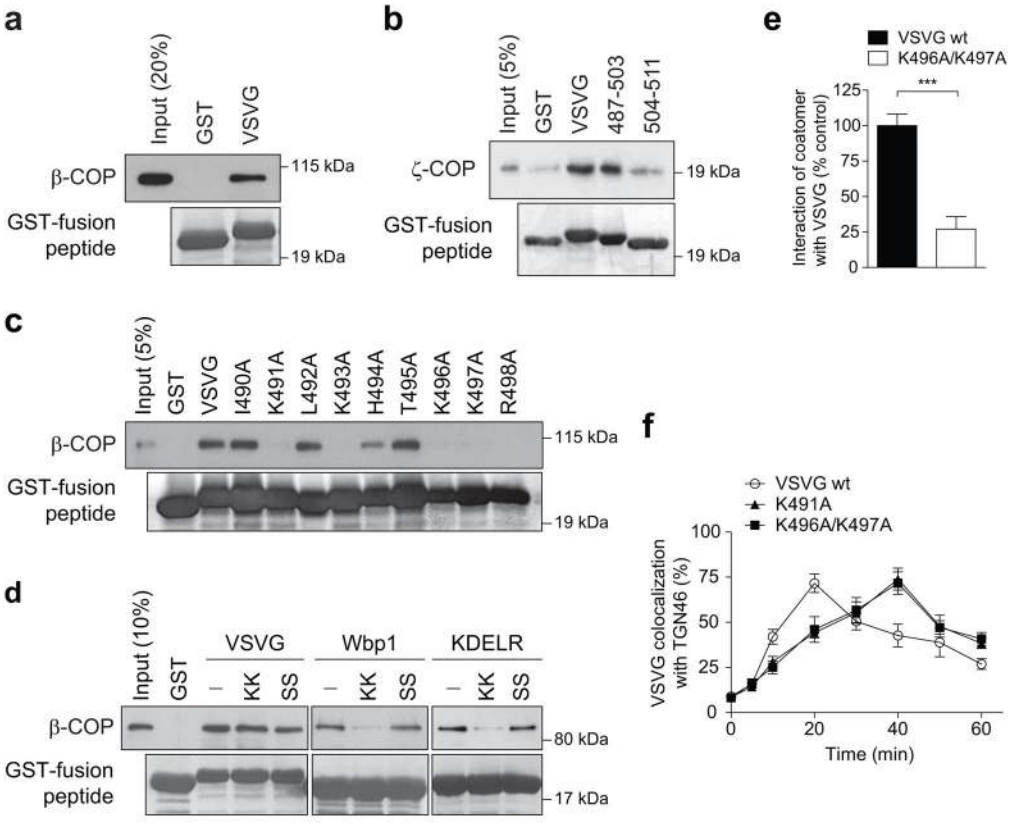

Figure 1. Coatomer binds VSVG to promote its transport through the Golgi

a-c, In vitro binding of the VSVG tail (**a**, full-length, **b**, truncations, **c**, point mutants) by coatomer, n = 3, **d**, Using the Wbp1 peptide that contains either the retrograde di-lysine motif (KK) or not (SS) for competition in cargo binding by coatomer, n = 4, **e**, FLIM examining VSVG interacting with coatomer, n = 3, mean +/− s.e.m., ***P<0.001 (two-tailed Mann-Whitney test), **f**, Effect of mutating the VSVG tail on its transport from ER to trans-Golgi, n = 4, mean +/− s.e.m.

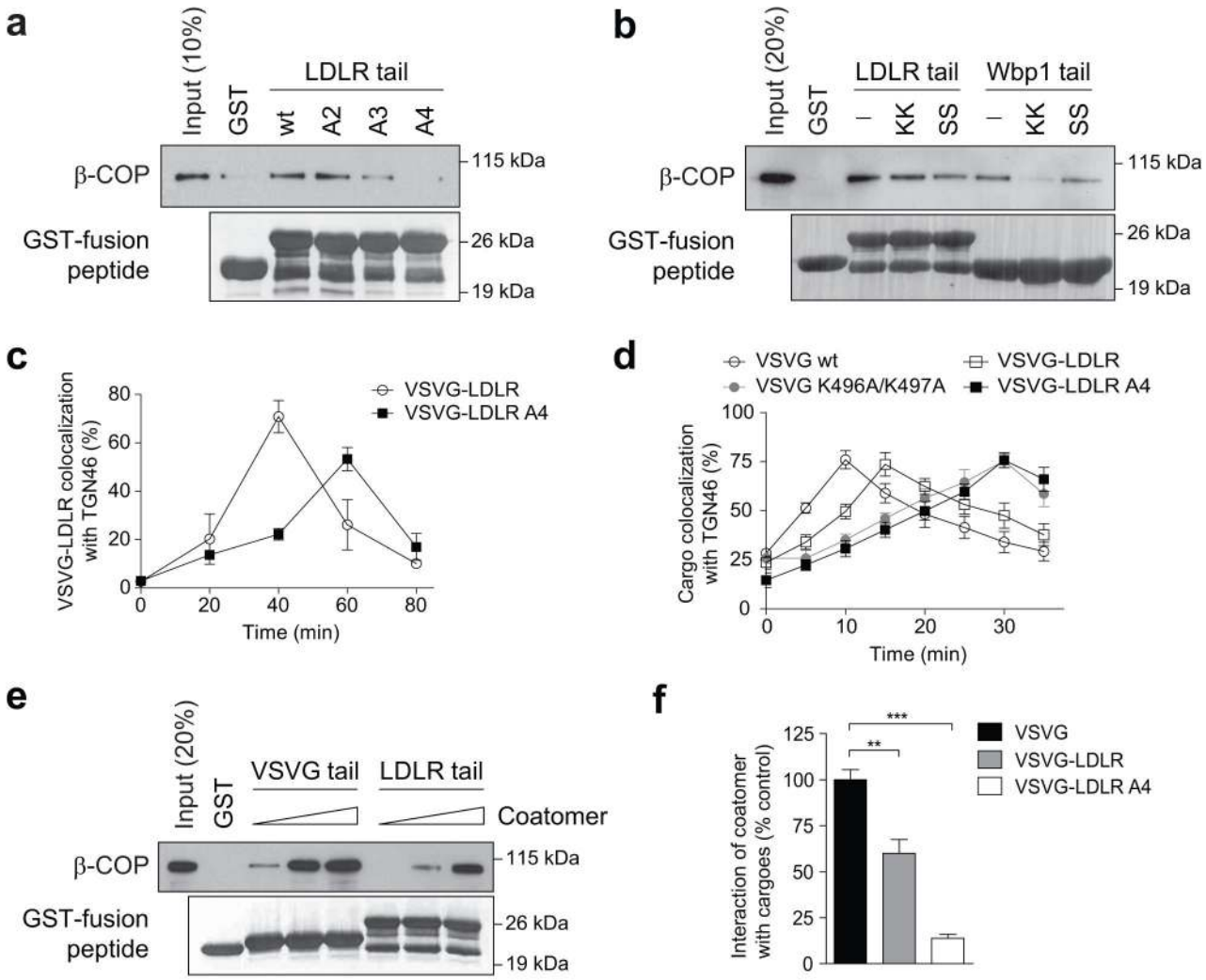

Figure 2. Coatomer also binds to the LDLR tail to promote the transport of VSVG-LDLR through the Golgi

a, In vitro binding of the LDLR tail (full-length and point mutants) by coatomer, n = 4, **b**, Using the Wbp1 peptides for competition in cargo binding by coatomer, n = 3, **c**, Effect of mutating the LDLR tail on the transport of VSVG-LDLR from ER to trans-Golgi, n = 4, mean +/− s.e.m. **d**, Effect of mutations in cargo tails on the intra-Golgi transport of different cargoes, n= 3, mean +/− s.e.m. **e**, Titrating coatomer level for in vitro binding to cargo tails, n = 2, **f**, FLIM examining different cargoes interacting with coatomer, n = 3, mean +/− s.e.m., **P<0.01, ***P<0.001 (two-tailed Mann-Whitney test).

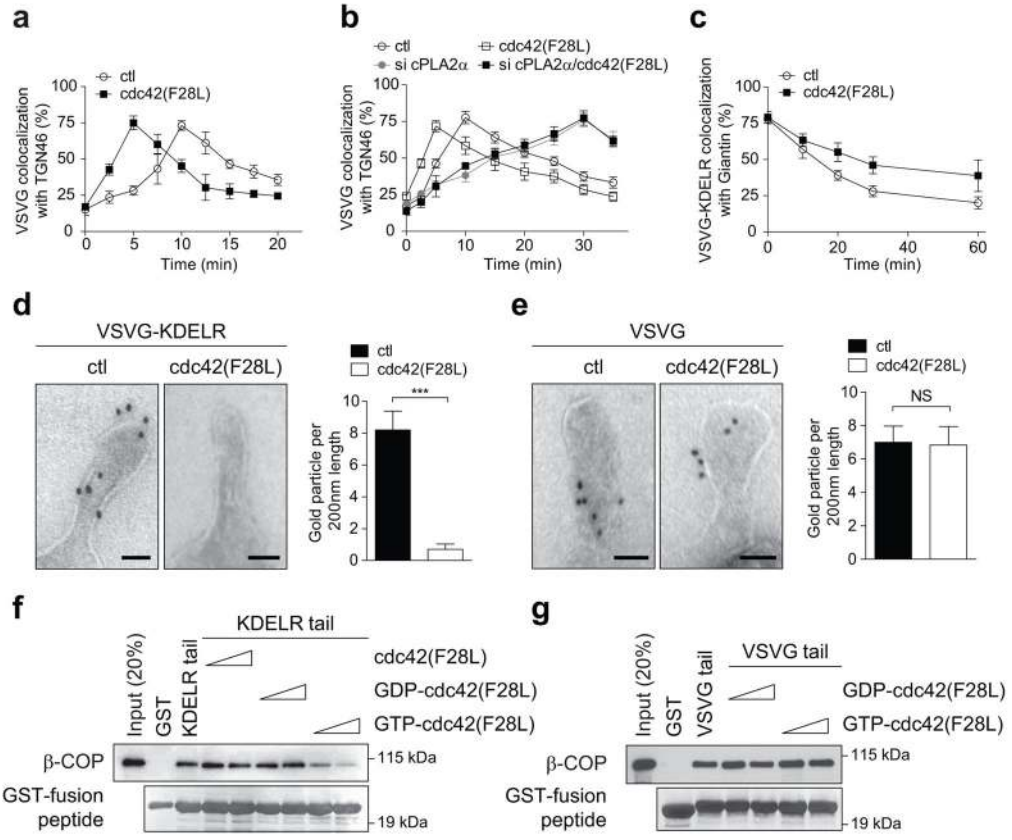

Figure 3. Cdc42 modulates cargo sorting by COPI

a,b, Effect of different conditions on the intra-Golgi transport of VSVG, n = 5, mean +/− s.e.m. **c,** Effect of expressing active cdc42 on VSVG-KDELR transport, n = 3, mean +/− s.e.m. **d, e,** Immunogold labeling of reconstituted COPI tubules, with representative (out of 15) EM images shown (bar = 50 nm), and also quantitation shown (n = 4, mean +/− s.e.m., ***P<0.001, NS indicating non-significance, two-tailed Student's *t*-test), **f, g,** Effect of adding different cdc42 forms on the binding of cargo tails by coatomer, n = 2.

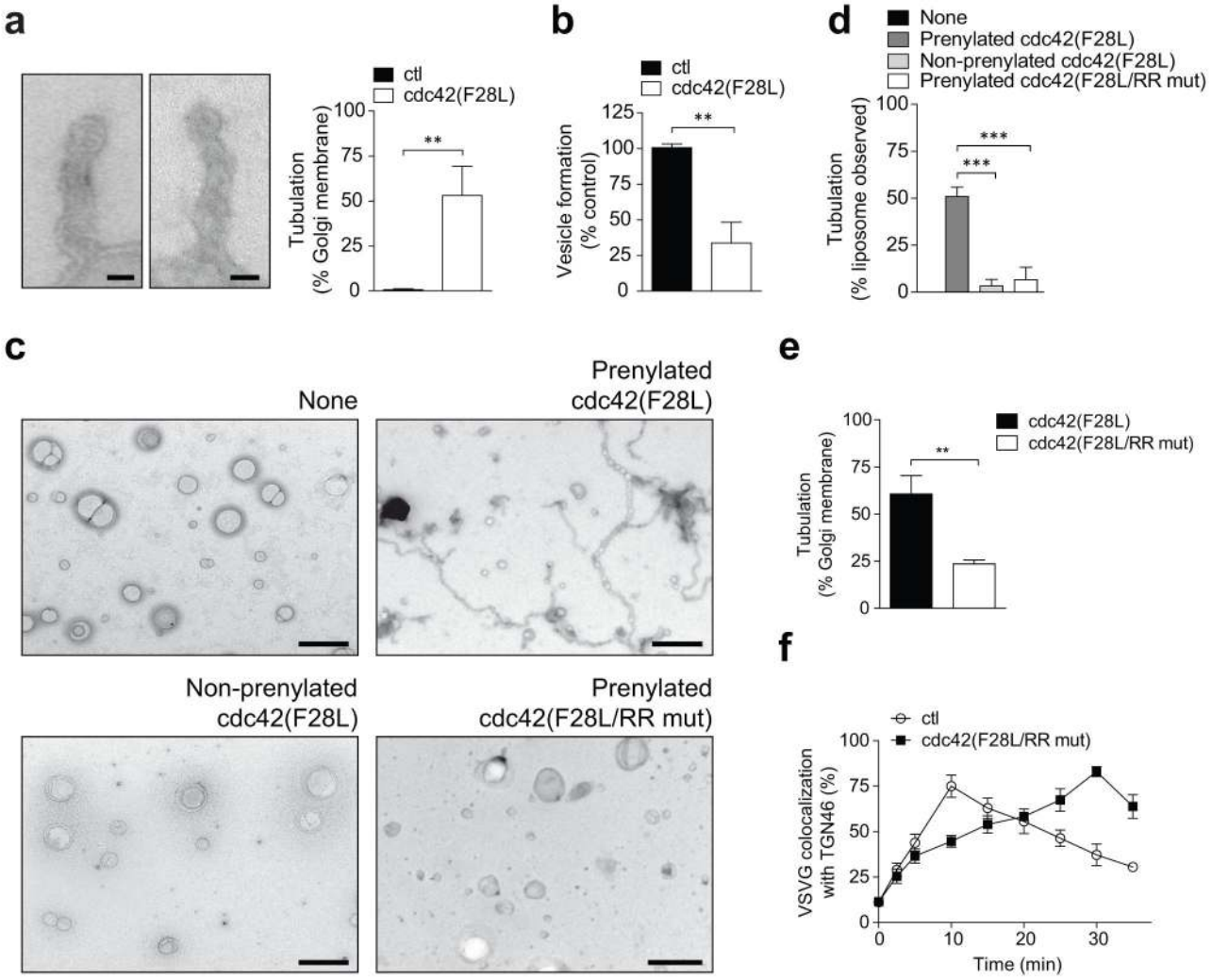

Figure 4. Cdc42 modulates carrier formation by COPI

a, Effect of active cdc42 on COPI tubule formation, with representative (out of 15) EM images shown (bar = 50 nm), and also quantitation shown (n = 4, mean +/− s.e.m., **P<0.01, two-tailed Student's *t*-test), **b**, Effect of active cdc42 on COPI vesicle formation, n = 6, mean +/− s.e.m., **P<0.01 (two-tailed Student's *t*-test), **c,d,** Effect of mutations in cdc42 on its ability to induce liposome tubulation, **c,** representative (out of 10) EM images (bar = 500 nm), **d,** quantitation (n = 5, mean +/− s.e.m., ***P<0.001, two-tailed Student's *t*-test), **e,** Effect of mutations in cdc42 on its ability to induce COPI tubule formation, n = 4, mean +/− s.e.m., **P<0.01 (two-tailed Student's *t*-test), **f,** Effect of mutations in cdc42 on its ability to promote the intra-Golgi transport of VSVG, n = 3, mean +/− s.e.m.